Finite Element Modeling of a Piezoelectric Composite Beam and Comparative Performance Study of Piezoelectric Materials for Voltage Generation

Nechibvute Action,[1] Chawanda Albert,[1] and Luhanga Pearson[2]

[1]*Physics Department, Midlands State University, P/Bag 9055 Gweru, Zimbabwe*
[2]*Physics Department, University of Botswana/Bag 0022, Gaborone, Botswana*

Correspondence should be addressed to A. Nechibvute at Midlands State University: nechibvutea@msu.ac.zw

A comparative study of the traditional PZT ceramics and new single crystals is critical in selecting the best material and optimiztion of transducer design for applications such as conversion of ambient vibrations into useful electrical energy. However, due to material and fabrication costs, and the need for rapid prototyping while optimizing transducer design, primary comparisons can be based on simulation. In this paper, the COMSOL Multiphysics finite element package was used to study the direct piezoelectric effect when an external load is applied at the free end of a piezoelectric composite beam. The primary output parameters such as electric potential and electric field where studied as a function of the input strain and stress. The modeling is presented for the relatively new single crystal lead magnesium niobate-lead titanate (PMN32) and three different lead zirconate titanate ceramics (PZT-5A, PZT-5H, PZT-4). Material performance was assessed by using a common geometry and identical excitation conditions for the different piezoelectric materials. For each material, there are three analyses performed, namely static, eigenfrequency and transient/time dependent analysis. Comparative results clearly suggest that the new crystal material PMN32 is capable of outperforming presently used piezoelectric ceramics for voltage generation.

1. Introduction

Piezoelectric materials have the novel ability of transferring electric to mechanical energy and vice-versa. This property is observable in many crystalline materials such as lead zirconate (PZT) ceramics where the phenomenon has found practical use in sensors and actuators [1-3]. Recently, the direct piezoelectric effect has been applied in energy harvesting where mechanical deformation on the piezoelectric material caused by ambient vibrations is converted to useful electrical energy [4-6]. The electrical energy is used to power ultra-low power electronics such as wireless sensor nodes and implantable biomedical devices [5-7]. The challenge facing piezoelectric energy harvesting is the low power output of the energy generators. One way of improving the direct piezoelectric effect and subsequently the energy harvesting capabilities of piezoelectric generators is the development of single crystal materials with high voltage generation abilities under low mechanical excitation compared to traditional PZT ceramics [8]. Understanding the direct piezoelectric performance of the PZT ceramic compared to new single crystal material such as PMN32 is very critical in the selection of the best material for a particular application. A detailed comparative study of different material performances is primarily inhibited by high material and fabrication costs and hence simulations in virtual design environments are required [9-11]. Finite element modeling (FEM) is an enabling tool that can allow detailed analysis of models and can predict the behaviour of electromechanical structures under real world conditions while enabling faster and cheaper prototype development [12,14]. In this study we model the direct piezoelectric effect on a composite beam consisting of a stainless steel substrate sandwiched between two piezoelectric layers using the commercial FEM software package COMSOL Multiphysics version 3.5, MEMS modules. With the geometry of the composite beam fixed, four different piezoelectric materials are used namely PZT-5A, PZT-5H, PZT-4 and PMN32. In each case three analyses were used: static, eigenfrequency and transient/time dependent. The static analysis was used to find the magnitudes and locations of maximum stress, strain and electrical potential of the

composite cantilever beam when a static load was applied to the beam's free end. The eigenfrequency analysis was then performed to find the first six modes of vibration and their associated mode shapes. Finally time dependent analysis was carried out to solve for the transient solution when the applied load was time dependent with a frequency matching and off the beam's first resonance frequency.

The paper is organized as follows: Section 2 presents the modeling of the composite beam, highlighting the equations governing the operation of the piezoelectric materials, the geometry, and procedures used in the COMSOL Multiphysics modeling environment. Section 3 gives a summary of the simulation results. Section 4 presents a brief discussion of the results and comparison of performance of PZT and PMN32 materials. Section 5 concludes the paper.

2. Modeling

2.1 Electromechanical model of a linear piezoelectric material and FEM. The stress-charge form of the electromechanical constitutive equations for linear piezoelectricity are given by [15]:

$$\mathbf{T} = \mathbf{c_E}\mathbf{S} - \mathbf{e}\mathbf{E}$$

$$\mathbf{D} = \mathbf{e^T}\mathbf{S} + \mathbf{\varepsilon_S}\mathbf{E} \tag{1}$$

where: **T** is the stress vector; **D** is the electric flux density vector, **S** is the strain vector; **E** is the electric field vector, c_E is the elasticity matrix (evaluated at constant electric field); e is the piezoelectric stress matrix, and ε_S is the dielectric matrix(evaluated at constant mechanical strain).

The equations in (1) represent the material behaviour which the FEM software solves for. The finite element discretization is performed by establishing nodal solution variables and the element shape functions over an element domain which approximates the solution [16]:

$$u_c = N_u^T.u \tag{2}$$

$$V_c = N_V^T.V \tag{3}$$

where: u_c is the displacement within element domain in the *x, y, z* directions; V_c is the electrical potential within element domain, N_u is the matrix of displacement shape functions, N_V is the vector of the electrical potential shape function, u is the vector of nodal displacements, and V is the vector of nodal electrical potential. Using Eqns. (2) and (3), the strain

S and electric field **E** are thus related to the displacements and potentials by eqns (4) and (5) respectively.

$$\mathbf{S} = B_u.u \tag{4}$$

$$\mathbf{E} = -B_V.V \tag{5}$$

where:

$$B_u = \begin{bmatrix} \dfrac{\partial}{\partial x} & 0 & 0 & \dfrac{\partial}{\partial y} & 0 & \dfrac{\partial}{\partial z} \\ 0 & \dfrac{\partial}{\partial y} & 0 & \dfrac{\partial}{\partial x} & \dfrac{\partial}{\partial z} & 0 \\ 0 & 0 & \dfrac{\partial}{\partial z} & 0 & \dfrac{\partial}{\partial y} & \dfrac{\partial}{\partial x} \end{bmatrix}^T \tag{6}$$

$$B_V = \begin{bmatrix} \dfrac{\partial}{\partial x} & \dfrac{\partial}{\partial y} & \dfrac{\partial}{\partial z} \end{bmatrix}^T \tag{7}$$

Upon the application of the variational principle and the finite element discretization, the coupled finite element matrix equation is:

$$\begin{bmatrix} M & 0 \\ 0 & 0 \end{bmatrix}\begin{bmatrix} \ddot{u} \\ \ddot{V} \end{bmatrix} + \begin{bmatrix} C & 0 \\ 0 & 0 \end{bmatrix}\begin{bmatrix} \dot{u} \\ \dot{V} \end{bmatrix} + \begin{bmatrix} K & K_z \\ K_z^T & K_d \end{bmatrix}\begin{bmatrix} u \\ V \end{bmatrix} = \begin{bmatrix} F \\ L \end{bmatrix} \tag{8}$$

where: M is the structural mass given by $M = \int \rho N_u N_u^T dv$; K is the structural stiffness given by $K = \int B_u^T c B_u dv$; K_z is the piezoelectric coupling matrix given by $K_z = -\int B_u^T e B_V dv$; K_d is the dielectric conductivity given by $K = \int B_V^T \varepsilon B_V dv$,C is the structural damping matrix; ρ is the mass density; F is the structural load vector (a vector of nodal forces, surface forces, and body forces); L is the electrical load vector (a vector of nodal, surface, and body charges). (The integration is over the whole element).

2.2 Geometry and modeling definition in COMSOL Multiphysics. The composite beam and its associated dimensions are shown in Figure 1 and Table 1 respectively. Throughout the modeling experiments in COMSOL Multiphysics-MEMS modules, the geometry and the dimensions shown in Figure 1 was not changed; only different piezoelectric materials where changed one type at a time. The material properties of the different piezoelectric materials are shown in Appendix 1.
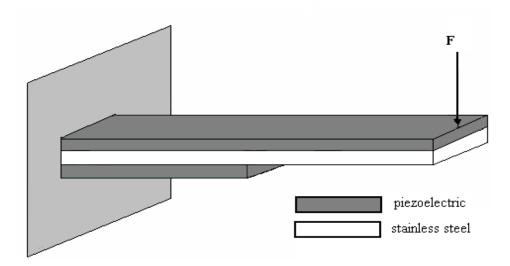
Figure 1: cantilever composite beam

TABLE 1: Dimensions of the composite beam.

Layer	Length (mm)	Width (mm)	Thickness (mm)
Top-piezoelectric	25	7.5	0.1
Middle-stainless steel	25	7.5	0.05
Bottom-piezoelectric	15	7.5	0.1

2.3 Model Procedures. To simulate the geometry in Figure 1, the piezo plane stress and plane stress where chosen as the Multiphysics problem in 2D. Appendix 1 shows the properties different materials retrieved from the COMSOL library [17] and used in the models. Two dimensional modeling (2D) was used instead of 3D because in 3D the very large number of elements caused the solver to consume a longer time to obtain a solution and in some cases failed to converge in the transient analysis [13, 18]. Furthermore 2D is more accurate than 3D analysis since it allows for the use of finer meshing size compared to coarse meshing employed in 3D.In the static analysis, the beam's free end is subjected to an arbitrarily chosen external load of load $F_X = 0$ and $F_Y = -10^5$ N/m^2. Inertial and damping effects are ignored. In the eigenfrequency analysis; the external load was removed and the model was submitted for analysis enabling the first six modes of vibration and their associated frequencies to be realized. Time-dependent analysis was performed to find the transient response to a harmonic load with the same

amplitude as the static load (i.e. a harmonic load $F_X = 0$ and $F_Y = -10^5 \sin(2\pi f t)$). The excitation frequency *(f)* was set to the first natural frequency found in the eigenfrequency analysis. In order to find the off-resonance performance of the composite beam; the analysis was also performed with the excitation frequencies below and above the first resonance values. Damping is very important in the analysis of time-dependent in order to get results that are as close to the real world as possible. The transient analysis model in COMSOL Multiphysics uses the Rayleigh damping given by: $C = \alpha_{dM} M + \beta_{dK} K$ where C, is the damping matrix, M, is the mass matrix, and K, is the stiffness matrix [17]. Throughout the transient analysis modeling, the damping coefficients α_{dM} and β_{dK} were set at 94.25 and 0.0001 respectively. The piezoelectric beam was meshed using the COMSOL Multiphysics standard meshing tool at 11160 triangular elements, and 65118 degrees of freedom.

3. Results Summary

Table 1: Summary of static analysis results

	Displacement (mm)	Von Mises Stress (MPa)	Strain x10³	Electric potential (V)	Electric Field norm (MV/m)	Electric energy density (J/m³)
PZT-5A	0.6434	38.33	0.5455	15.8335	0.6627	1508.2
PZT-5H	0.625	39.96	0.5455	12.702	0.5225	1748.524
PZT-4	0.5	37.85	0.4129	14.9615	0.6146	1098.351
PMN32	1.59	38.26	1.382	18.0223	0.5399	3785.961

TABLE 2: Summary of eigenfrequency analysis results

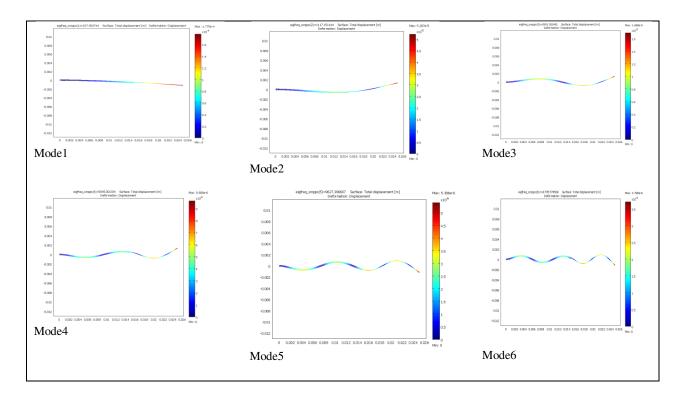|	*f1/Hz*	*f2/Hz*	*f3/Hz*	*f4/Hz*	*f5/Hz*	*f6/Hz*
PZT-5A	237.503744	1117.15114	2991.352491	5945.001334	9627.396607	14705.579508
PZT-5H	243.85559	1145.492784	3067.62181	6096.261632	9873.353056	15082.978781
PZT-4	274.079525	1263.173713	3391.705788	6723.378674	10903.812945	16655.978892
PMN32	146.877937	728.170014	1952.253729	3878.945263	6304.482396	9575.683795

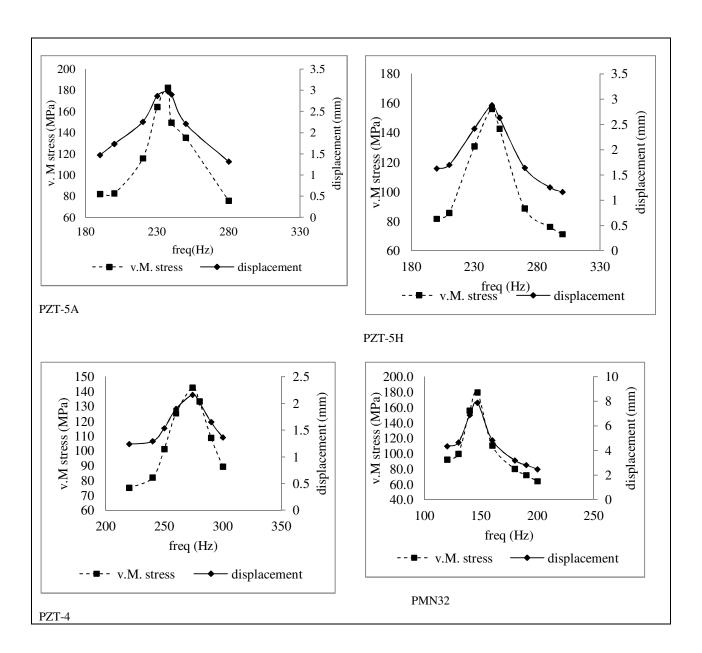FIGURE 2: The first six deformation modes of the composite piezoelectric, using PZT-5A

FIGURE 3: Plots of von Mises stress and displacement as a function of excitation frequency
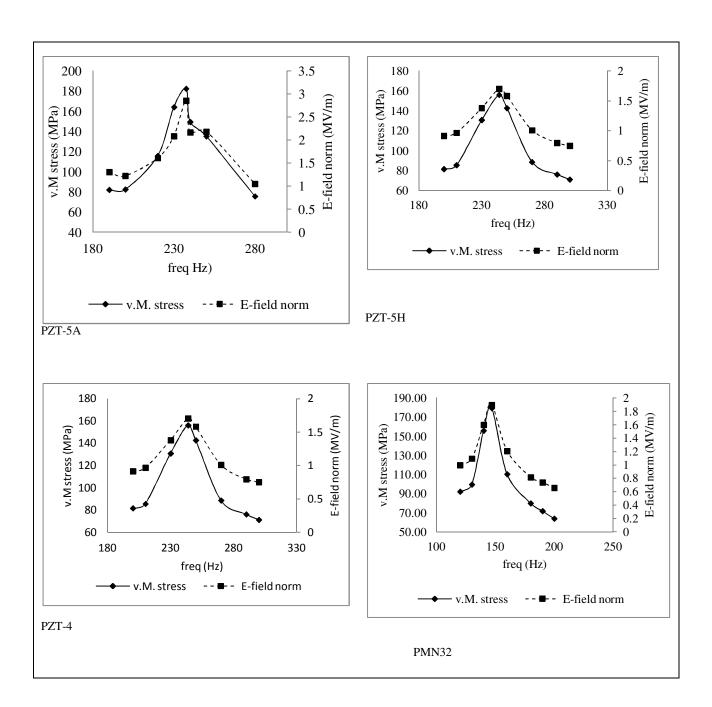
FIGURE 4: Plots of von Mises stress and electric field-norm as a function of excitation frequency
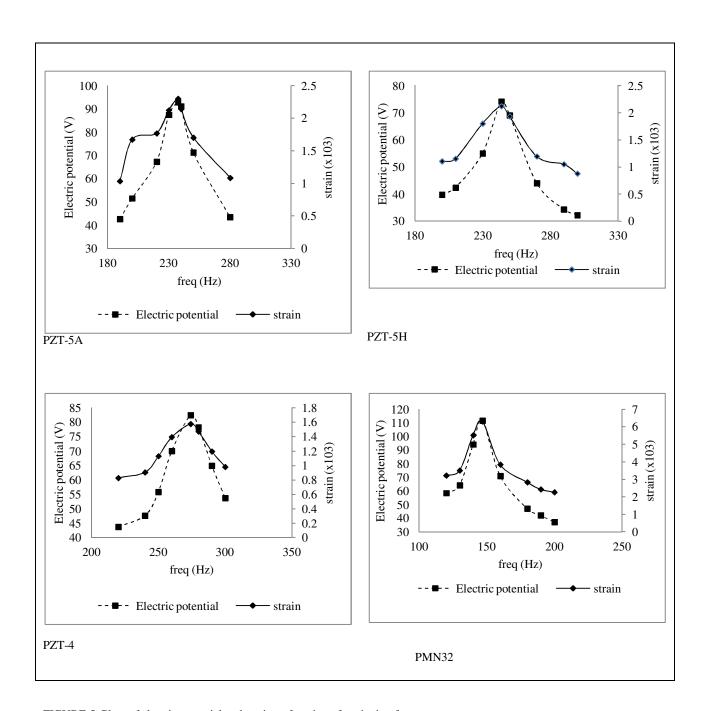
PZT-5A

PZT-5H

PZT-4

PMN32

FIGURE 5: Plots of electric potential and strain as function of excitation frequency

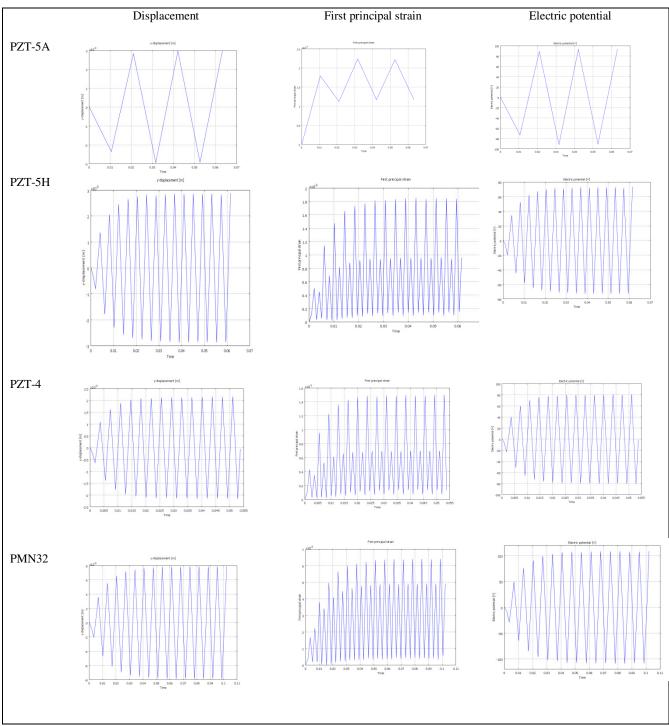|	Displacement	First principal strain	Electric potential
PZT-5A			
PZT-5H			
PZT-4			
PMN32			

FIGURE 6: Displacement, strain and electric potential profiles for the different material models (at first resonance frequency)
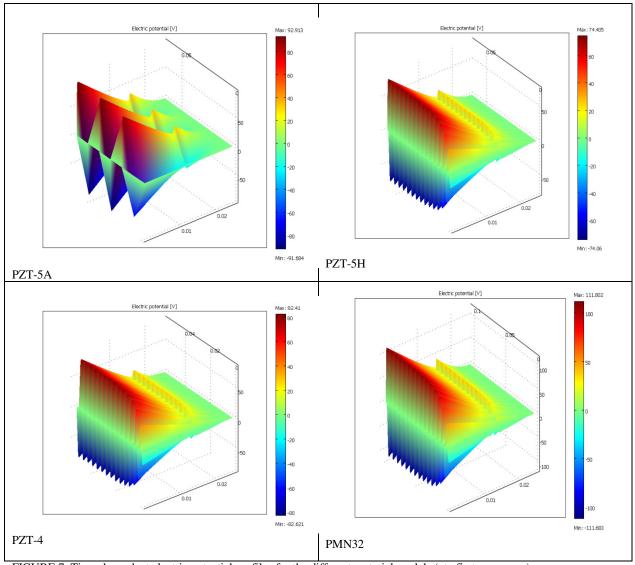
FIGURE 7: Time-dependent electric potential profiles for the different material models (at first resonance)

4. Results Analysis, Discussion and Comparison of Performance

The consistency in the values of the applied load, composite beam geometry, and boundary conditions used in the FEM study laid a strong basis to allow fair comparison of results from the static and time dependent analyses for the four types of piezoelectric material models. The results of static analysis in Table 3 show that with a static load of 100 kN/m^2, the model which consists of PMN32 material gave the highest electric potential of 18.0223 V. The model with PZT-5A gave the second highest electric potential of 15.8335 V, that consisting of PZT-4 was third with 14.9615 V whereas PZT-5H model ranked fourth with a potential of 12.702 V. As may be expected from the direct piezoelectric effect, the material model with the highest electric potential is also the one with the highest electric energy density, von Mises stress, first principal strain and beam displacement. In addition, the static analysis confirmed that strain and electric potential are maximum at the beam's fixed end reduce in value as one traverses towards the free end of the beam (APPENDIX 2). Generally, the static analysis suggests that for the studied geometry, PMN32 exhibits strongest direct piezoelectric performance relative to PZT ceramics in terms of voltage generation.

The results of eigenfrequency analysis presented in Table 4 were used set up the excitation frequency of the time –dependent load in the transient analysis. The eigenfrequency analysis reveals that the PZT-4 material model has the highest first resonance frequency of 274.08Hz, followed by PZT-5H with 243.86Hz, PZT-5A with 237.50 Hz and PMN32 material model has the lowest first resonance frequency of 146.88Hz. Guided by the values of the first resonance frequencies, time-dependent analysis using the same magnitude for the dynamic load was performed for the different material models and the plots in Figures 3-5 show the strong frequency dependence of the key electrical and mechanical parameters in the direct piezoelectric property of the materials. Time-dependent results show that stress, strain, electric field and electrical potential are at their maximum values at the first resonance; the values of these quantities decrease as the excitation

frequency deviates from the resonance frequency. The model which consists of PM32 material gave the highest electric potential of 111.7425V,followed by PZT-5A with 92.982V, that consisting of PZT-4 was third highest with 82.51 and PZT-5H model gave the lowest potential of 74.2325V. Figure 7 shows the electric potential distribution along the composite beam's top surface. From the figure it is observed that the electric potential is highest at the beam's fixed end, and change from maximum to minimum with respect to time. This is in excellent agreement with expectation from the direct piezoelectricity relationship: the maximum electric potential exists at the area that has maximum strain. The relative performance comparison is presented in Figure 7. These results confirm the superior performance of PMN32 over PZT ceramics as has been reported by the work of other researchers [10, 19-20].
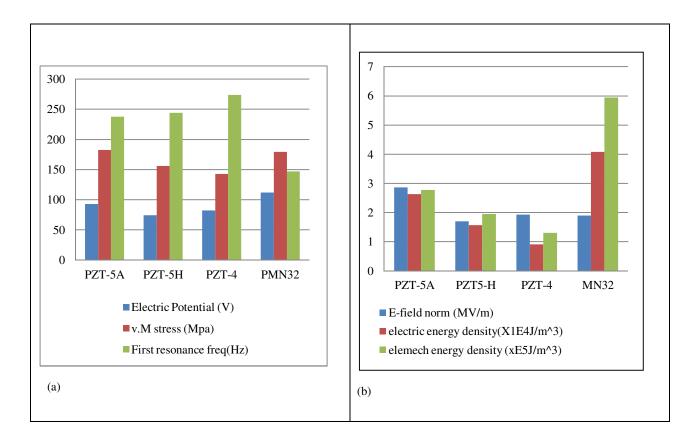

FIGURE 8: Relative performance comparison of the four piezoelectric material models

5. Conclusion

In this paper, FEM using he commercial COMSOL Multiphysics package was used to study performance of a composite piezoelectric beam. For both static and time dependent mechanical excitations, simulation results have shown that PM32 has the highest greatest voltage generation ability. PZT-5A was a close second, followed by PZT-4 in the third rank while PZT-5H ranked forth with the lowest electric potential. In addition to the largest values of the electrical potential, the PMN32 material model also gave the highest average values of electric field, electric energy density, stress, strain, and displacement. On the other hand, PMN32 material model has lowest first resonance frequency of compared to the PZT models. As future research, the strong piezoelectric effect demonstrated by PMN32 needs to the further studied, particularly in the context of vibration to electric power generation to enable optimization of the material properties and design geometry of the cantilever device.

References

[1] P. Muralt, "Ferroelectric thin films for micro-sensors and actuators: a review," *Journal of Micromechanics and Microengineering*, vol.10 pp.136–146, 2000.

[2] C. Niezrecki, D. Brei, S. Balakrishnan and A. Moskalik, "Piezoelectric Actuation: State of the Art," *The Shock and Vibration Digest*, vol. 33, no. 4, pp. 269-280, 2001.

[3] J. F. Tressler, S. Alkoy and R. E. Newnham, "Piezoelectric Sensors and Sensor Materials," *Journal of Electroceramics*, vol.2, no.4, pp. 257-272, 1998

[4] S.R. Anton and H.A. Sodano, "A review of power harvesting using piezoelectric materials (2003-2006)," *Smart Materials and Structures*, vol. 16, pp. R1,2007

[5] K. A. Cook-Chennault , N. Thambi and A. M. Sastry, "Powering MEMS portable devices-a review of non-regenerative and regenerative power supply systems with special emphasis on piezoelectric energy harvesting systems," *Smart Materials and Structures,* vol.17, no.4, pp.043001, 2008.

[6] S. P. Beeby , M. J. Tudor and N. M. White, "Energy harvesting vibration sources for microsystems applications," *Measurement Science and Technology*, vol. 17, no. 2, pp.R175 - R195 , 2006.

[7] M. P. Buric, G. Kusic, W. Clark and T. Johnson, "Piezo-electric energy harvesting for wireless sensor networks," in *Proceedings of Wireless and Microwave Conference, WANICON IEEE Annual*, pp. 1-5,4-5 December 2006,

[8] D. Guyomar and M. Lallart, "Recent Progress in Piezoelectric Conversion and Energy Harvesting Using Nonlinear Electronic Interfaces and Issues in Small Scale Implementation," *Micromachines*, vol.2, pp. 274-294, 2011.

[9] P. Marin-Franch, S. Cochran, and K. Kirk, "Progress towards ultrasound applications of new single crystal materials," *Journal of Material Science: Materials in Electronics*, vol. 15, pp. 715-720, 2004.

[10] I. A. Ivan , M. Rakotondrabe,J. Agnus, R. Bourquin ,N. Chaillet , P. Lutz , J.-C. Poncot, R. Duffait and O. Bauer, "Comparative material study between PZT ceramic and newer PMN-PT and PZN-PT materials for composite bimorph actuators," *Reviews on Advanced Materials,* vol 24, no 1/2, pp.1-9, 2010.

[11] E. Aksel and J. L. Jones, "Advances in Lead-Free Piezoelectric Materials for Sensors and Actuators,' *Sensors ,*vol 10, pp. 1935-1954, 2010.

[12] H. Allik, T. J. R. Hughes, "Finite Element Method for Piezoelectric Vibrations," *International Journal for Numerical Methods in Engineering*, vol 2, pp. 151-157, 1970.

[13] V. Piefort, *Finite Element Modeling of Piezoelectric Active Structures*, Doctoral Thesis, University of Brussels, pp. 51–69, 2001.

[14] A. Benjeddou, "Advances in piezoelectric finite element modeling of adaptive structural elements: a survey," *Computers and Structures*, vol. 76, pp.347-363, 2000.

[15] IRE, *Standard on piezoelectric crystals: Determination of the elastic, piezoelectric and dielectric constant*, 58 IRE 14, 1962.

[16] D. Popovici, F. Constantinescu, M. Maricaru, F. I. Hantila, M. Nitescu and A. Gheorghe, "Modeling and Simulation of Piezoelectric Devices," in Modeling and Simulation edited by G. Petrone and G. Cammarata, Intech, ,Intech, pp. 472-500, 2008.

[17] COMSOL Multiphysics, version 3.5 Release Documentation,www.comsol.com

[18] M. Emam, *Finite element analysis of composite piezoelectric beam using Comsol*, Masters Thesis, Drexel University, 2008

[19] S. R. Anton, *Multifunctional piezoelectric energy harvesting concepts*, PhD Thesis, Virginia Polytechnic Institute and State University, 2011

[20] C. Green, K.M. Mossi and R.G. Bryant, "Scavenging Energy from piezoelectric materials for wirelss sensor applications," in *Proceedings of ASME International Mechanical Engineering Congress and Exposition, IMCE2005*, pp. 5-11, Orlando, Florida, USA, November 2005.

APPENDIX 1: Piezoelectric Material Properties

1. Elasticity matrix (C_E), X 10^{10}Pa	

$$\begin{bmatrix} 12.0346 & 7.51791 & 7.50901 & 0 & 0 & 0 \\ 7.5191 & 12.0346 & 7.50901 & 0 & 0 & 0 \\ 7.50901 & 7.50901 & 11.0867 & 0 & 0 & 0 \\ 0 & 0 & 0 & 2.10526 & 0 & 0 \\ 0 & 0 & 0 & 0 & 2.10526 & 0 \\ 0 & 0 & 0 & 0 & 0 & 2.25734 \end{bmatrix}$$

PZT-5A

$$\begin{bmatrix} 12.7205 & 8.02122 & 8.46702 & 0 & 0 & 0 \\ 8.02122 & 12.7205 & 8.46702 & 0 & 0 & 0 \\ 8.46702 & 8.46702 & 11.7436 & 0 & 0 & 0 \\ 0 & 0 & 0 & 2.29885 & 0 & 0 \\ 0 & 0 & 0 & 0 & 2.29885 & 0 \\ 0 & 0 & 0 & 0 & 0 & 2.34742 \end{bmatrix}$$

PZT-5A

$$\begin{bmatrix} 13.8999 & 7.78366 & 7.42836 & 0 & 0 & 0 \\ 7.78366 & 13.8999 & 7.42836 & 0 & 0 & 0 \\ 7.42836 & 7.42836 & 11.7436 & 0 & 0 & 0 \\ 0 & 0 & 0 & 2.564 & 0 & 0 \\ 0 & 0 & 0 & 0 & 2.5641 & 0 \\ 0 & 0 & 0 & 0 & 0 & 3.0581 \end{bmatrix}$$

PZT-4

$$\begin{bmatrix} 13.3 & 9.85 & 9.63 & 0 & 0 & 0 \\ 9.85 & 13.3 & 9.63 & 0 & 0 & 0 \\ 9.63 & 9.63 & 10.2 & 0 & 0 & 0 \\ 0 & 0 & 0 & 7.14 & 0 & 0 \\ 0 & 0 & 0 & 0 & 7.14 & 0 \\ 0 & 0 & 0 & 0 & 0 & 6.67 \end{bmatrix}$$

PMN32

2. Coupling matrix (e),C/m^2

$$\begin{bmatrix} 0 & 0 & 0 & 0 & 12.2947 & 0 \\ 0 & 0 & 0 & 12.2947 & 0 & 0 \\ -5.35116 & -5.35116 & 15.7835 & 0 & 0 & 0 \end{bmatrix}$$

PZT 5A

$$\begin{bmatrix} 0 & 0 & 0 & 0 & 17.0345 & 0 \\ 0 & 0 & 0 & 17.0345 & 0 & 0 \\ -6.62281 & -6.62281 & 23.2403 & 0 & 0 & 0 \end{bmatrix}$$

PZT-5H

$$\begin{bmatrix} 0 & 0 & 0 & 0 & 12.7179 & 0 \\ 0 & 0 & 0 & 12.7179 & 0 & 0 \\ -5.20279 & -5.20279 & 15.0804 & 0 & 0 & 0 \end{bmatrix}$$

PZT-4

$$\begin{bmatrix} 0 & 0 & 0 & 0 & 13.57143 & 0 \\ 0 & 0 & 0 & 13.57143 & 0 & 0 \\ -3.7795 & -3.7795 & 25.68634 & 0 & 0 & 0 \end{bmatrix}$$

PMN32

3. Relative permittivity, ε_{rs}

$$\begin{bmatrix} 919.1 & 0 & 0 \\ 0 & 919.1 & 0 \\ 0 & 0 & 826.6 \end{bmatrix}$$

PZT-5A

$$\begin{bmatrix} 1704.4 & 0 & 0 \\ 0 & 1704.4 & 0 \\ 0 & 0 & 81433.6 \end{bmatrix}$$
PZT-5H

$$\begin{bmatrix} 762.5 & 0 & 0 \\ 0 & 762.5 & 0 \\ 0 & 0 & 663.2 \end{bmatrix}$$

PZT-4

$$\begin{bmatrix} 3309 & 0 & 0 \\ 0 & 3309 & 0 \\ 0 & 0 & 1264 \end{bmatrix}$$

PMN32

4. Mass density (ρ),kg/m^3

PZT-5A	PZT-5H	PZT-4	PMN32
7750	7500	7500	8040

APPENDIX 2: Static Analysis Profiles for different piezoelectric material models

	Displacement	First principal strain	Electric potential
PZT-5A			
PZT-5H			
PZT-4			
PMN32			